Physiological and Molecular Plant Pathology 62 (2003) 155–166

PMPP

www.elsevier.com/locate/pmpp

Ultrastructural comparison of a compatible and incompatible interaction triggered by the presence of an avirulence gene during early infection of the smut fungus, *Ustilago hordei*, in barley

G.G. Hu, R. Linning, G. Bakkeren*

Pacific Agri-Food Research Centre, Agriculture and Agri-Food Canada, Summerland, Canada BC VOH 1Z0

Accepted 5 March 2003

Abstract

Cell morphologies and reactions during infection of barley by the smut fungus, *Ustilago hordei*, were investigated by TEM. We compared compatible and incompatible interactions caused respectively by the absence or presence of an avirulence gene (V1) on cultivar 'Hannchen', harboring the cognate resistance gene (*Ruh1*). In both interactions, *U. hordei* penetrated coleoptile epidermal cells directly within two days post inoculation (dpi). Upon penetration, an electron-opaque interfacial matrix formed around both inter- and intracellular hyphae in compatible interactions. Hyphae grew and extended into the host bundle sheath and invaded parenchyma cells. At 12 dpi, cell wall appositions formed surrounding the hyphae. Tubule-like structures of variable thickness and orientation were visible in the interfacial matrix mainly in the outer region bordering these appositions. In contrast, in incompatible interactions, cell wall appositions occurred as soon as hyphae penetrated host epidermal cells. Material, thicker and more granular in appearance compared to that in compatible interactions, was deposited around the invading hyphae and extended onto the inner surface of invaded epidermal cells. Upon penetration, host cell reactions included disorganization of cytoplasm and organelles leading to necrosis and cell death. This gene-for-gene combination triggers a very early hypersensitive response-like resistance reaction, extremely localized at sites of primary infection which involves only a few plant cells and may or may not be responsible for fungal arrest.

Keywords: Avirulence gene; Cell wall apposition; *Hordeum vulgare*; HR; Necrosis; Ultrastructure

1. Introduction

Ustilago hordei (Pers. Lagerh.) causes the economically significant disease of covered smut on barley and oats. The fungus has a worldwide distribution and effective control is currently through the use of resistant cultivars or application of seed dressings [9, 27, 39, 40]. In regions where chemical approaches are restricted, unavailable or uneconomical, the planting of resistant cultivars is the only option to control the disease. Moreover, the pathogen may also develop a tolerance to fungicides, further increasing the value of cultivars resistant to the fungus [42]. In most monoculture settings, control has relied on single gene resistance creating the potential for epidemic outbreaks [39].

In smut fungi such as *U. hordei*, fusion of haploid basidiospores of opposite mating types is an essential step in the life cycle [9]. This sporidial mating is controlled by a single mating type locus (*MAT*) with two known alternative alleles, *MAT-1* (formerly called *A*) and *MAT-2* (formerly called *a*; [3,4,23,39]). These fusion events also bring together avirulence alleles that determine compatibility or incompatibility during the interaction with the host. Classical genetic studies have identified six avirulence genes in *U. hordei* which in different combinations make up at least 17 different races. Six corresponding resistance genes have been found in the various differential barley cultivars [1,8,30,31,35,36].

The dikaryon resulting from mating is the obligate parasitic, mycelial cell type of this hemibiotrophic fungus which needs the host for survival and to complete its life cycle. Our laboratory has previously reported on

* Corresponding author. Tel.: +1-250-494-6368; fax: +1-250-494-0755.
E-mail address: bakkereng@agr.gc.ca (G. Bakkeren).

0885-5765/03/$ - see front matter
doi:10.1016/S0885-5765(03)00037-7

the complete infection process of the smut fungus, *Ustilago hordei*, in a compatible barley plant [17]. After penetrating epidermal cells directly through an appressorium-like structure, hyphae colonized intercellular spaces and moved between mesophyll cells. We demonstrated that the growth of mycelium in plant tissue was both intra- and intercellular, although it appeared that after penetration the former mode was prevalent [10]. Although intracellular hyphae were consistently encased by cell wall apposition, there was no significant difference in morphology between intra- and intercellular hyphae. Hyphae grew directly, without much branching, perpendicular to the long axis towards the meristematic region as if responding to a chemical gradient. They established themselves in or just below the shoot meristem where the fungus resided until differentiation of this meristem into floral tissue. During the whole process no recognizable damage was introduced. Plant cells often remained viable after penetration illustrating the intimate biotrophic relationship this fungus establishes with its host. The fungus proliferated in the developing spikelets of the inflorescence and upon emergence, barley kernels of susceptible plants had been replaced with masses of black sooty teliospores [17,21,42]. Numerous nutritional and environmental factors may also modulate the process [26].

Macroscopically, susceptibility is indistinguishable from resistance until heading of the plant. The point at which susceptible and resistant reactions diverge has been difficult to determine due to the absence of detectable symptoms in the former case and a lack of a visible host defense response such as a hypersensitive response (HR) or HR in the latter. Little is known about how or when the infection process is blocked in incompatible or resistant *U. hordei*–barley interactions and no detailed cytological studies are available on small grain-infecting smuts involving race-cultivar resistance. In separate histological studies, Kiesling [19] and Chatterjee [7] used light microscopy to study the interaction of *U. hordei* race 6 on four barley cultivars ranging from susceptible to intermediate and fully resistant. They reported some anatomical changes, such as the formation of a 'sheath' around hyphae penetrating epidermal cells and tissues of resistant barley varieties, and also the collapse of these invaded cells. Both studies concluded that a common expression of incompatibility was simply the failure of the hyphae to grow into the primordia of the host seedling.

This study provides a detailed, ultrastructural description of mycelial development and host cell reactions during the early stages of the infection process in an incompatible interaction resulting from a specific gene-for gene combination. We compare these processes with those during a compatible interaction. The possible contribution of ultrastructural features during the host cell responses to the resistance of *U. hordei* infection will be discussed.

2. Materials and methods

2.1. Fungal strains and inoculations

U. hordei strains used originate from Canadian Prairies teliospore collections, #4854 (*v1v1*) and #4857 (*V1V1*), both homozygous for avirulence gene *V1* ([37,38]; J. Menzies, Cereal Research Centre, AAFC, Winnipeg, Manitoba, Canada). Mated strains of genotype *v1v1* will infect barley cultivar 'Hannchen' harboring resistance gene *Ruh1* and produce teliospores in up to 70% of the plants under greenhouse conditions. This is the compatible interaction in this gene-for-gene system. Mated strains of genotype *V1V1* or *V1v1* will not produce teliospores on barley cultivar 'Hannchen', the incompatible interaction. Uh359 (*v1MAT-1*) and Uh362 (*v1MAT-2*) are progeny from collection #4854 and Uh381 (*V1MAT-1*) and Uh415 (*V1MAT-2*) are progeny from a cross between segregants from #4854 (*v1v1*) and #4857 (*V1V1*).

Strains were cultured on potato dextrose agar (PDA) plates at 22°C. Single colonies were transferred into liquid potato dextrose broth (PDB) and grown while shaking at 22°C until cultures reached mid-log phase. The sporidia were collected by centrifugation for 5 min at 3000***g*** and then resuspended in sterile double distilled water at a density of 1×10^6 cells ml^{-1}. A cell suspension inoculum was prepared by mixing equal amounts of cells of opposite mating type. Seeds of cv. 'Hannchen' were dehulled and surface sterilized for 1 min in 70% EtOH, followed by 10 min in 1% NaOCl and several washes with sterile, double-distilled water. They were subsequently allowed to germinate under sterile conditions in petri dishes lined with water-soaked filter paper at 22°C in a dark incubator. At 48 h, roots had emerged from the barley seedlings and shoots varied in size from 5 to 15 mm. At that point, inoculum was applied gently with sterile cotton-wrapped stubs to the surface, approximately 5 mm wide, around the crown area and anticipated meristematic region. Inoculated seeds in petri dishes were overlaid with moist, sterile filter paper and kept dark in a moist chamber at 21°C. Shoots from treated seeds continued to elongate; at 6 dpi, 1–2 leaves had extended completely and at 12 dpi, 3–4 leaves had extended completely. Samples from inoculated regions around the anticipated meristem were collected at 2 days post inoculation (dpi) from the coleoptile. At six and 12 dpi this coleoptilar region seemed to have developed into a leaf base. These samples were then processed for transmission electron microscopy.

2.2. Sample processing for transmission electron microscopy (TEM)

Samples for microscopic analysis were prepared as described in Hu and Rijkenberg [15]. Briefly, the harvested shoots were sliced into 3 mm × 3 mm pieces and fixed in 3% glutaraldehyde in 0·05 M sodium cacodylate buffer, pH 7·2 (CB) overnight. Subsequently the samples were

washed twice in CB, postfixed for 2 h in 2% osmium tetroxide in CB at room temperature, rewashed in CB, and then dehydrated in a graded ethanol series. The samples were then embedded in Spurr's resin [34]. Ultrathin sections were obtained by cutting with a diamond knife and stained by soaking in 2% uranyl acetate for 15 min. The sections were then washed in double-distilled water, post-stained in lead citrate for 15 min, and finally washed again in double-distilled water. Ultrastructure analysis was performed with a Jeol 100CX transmission electron microscope at 80 kV. TEM images were made by digitizing the black and white photographic negatives. Adobe Photoshop 6·0 was used to adjust image contrast and to compose all plates.

3. Results

3.1. Compatible interaction between barley and U. hordei

A detailed study of mating interactions between *U. hordei* cells on the barley shoot surface, direct penetration through appressorium-like structures, and of the complete subsequent infection cycle has been described for a compatible interaction by our laboratory [17]. At 2 days after inoculation (dpi), infective hyphae had penetrated into the young barley shoot and seemed to grow in tissues both inter- and intracellularly [10,17]. In many cases there was a thin layer of electron-opaque substance around the hyphal wall of young intracellular mycelium (Fig. 1), which was called the 'interfacial matrix' in this study after Luttrell [25]. Nuclei, mitochondria, endoplasmic reticula, Golgi bodies, lipid bodies and vacuoles were evident in the fungal cytoplasm.

The fungus progressed without much branching, occasionally invading bundle sheath cells (such as parenchyma cells at 6 dpi; Figs. 2 and 3). At this stage a thick electron-opaque interfacial matrix was found between plant plasma membranes and fungal cell walls (Fig. 2). However, the plant plasma membrane was continuous and not damaged by the fungal invasion (Figs. 2 and 3). In the contact region between fungal mycelium and plant cell wall, the electron-opaque substance seemed to infiltrate the host cell wall (Fig. 3).

Cell wall apposition, which seemed continuous with the plant cell wall, was present adjacent to the electron-opaque substance (Fig. 4). The texture of the cell wall appositions appeared to be uniform, but occasionally, granular-appearing vesicles were observed inside (Fig. 4). Cell wall appositions usually occurred during the later stages of fungal development around 12 dpi in plant tissues surrounding the penetrating hyphae (Figs. 5 and 6) or extended into plant cytoplasm (Fig. 7). These appositions usually formed from the inner surface of the host cell wall, without breaking the host plasma membrane, and extended to cover the whole invading hyphae (Figs. 5 and 6). In the intercellular space in the bundle sheath, interfacial matrix but not cell wall apposition was present around the fungal mycelium (Fig. 8). Septa were observed in both inter- and intracellular hyphae (Fig. 9). At 12 dpi, the fungus had spread into regions close to the meristematic growing point of the plant [17].

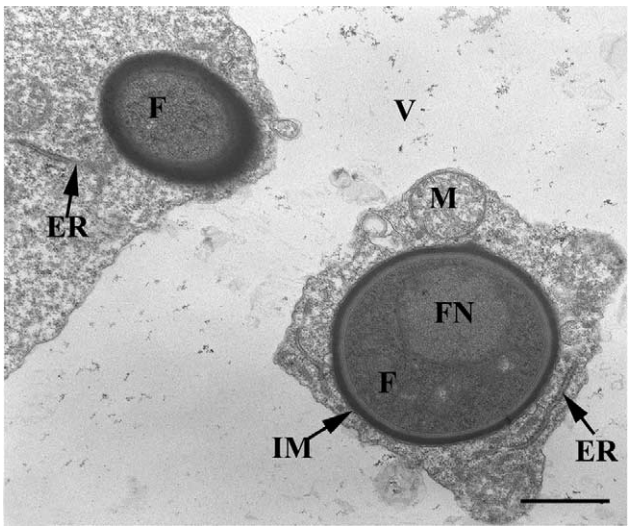

Fig. 1. Transmission electron micrograph of a compatible interactions between *U. hordei* and barley. Two days post inoculation (2 dpi). The thin interfacial matrix surrounded the young hypha in plant cytoplasm (arrows). Scale bar = 1 μM. Abbreviations: A: appressorium; CWA: cell wall apposition; Ep or Ec: epidermal cell; EpW; epidermal cell wall; ER: endoplasmic reticulum; F: hypha; FN: fungal nucleus; G: Golgi body; HC: host cell; IM: interfacial matrix; IS: intercellular space; M: mitochondrion; Mc: mesophyll cell; NPC: necrotic plant cell; OS: osmiophillic substance; Pa: parenchyma cell; PN: plant nucleus; PW: plant cell wall; Se: fungal septum; V: vacuole; Ve: vesicle; Xy: xylem cell.

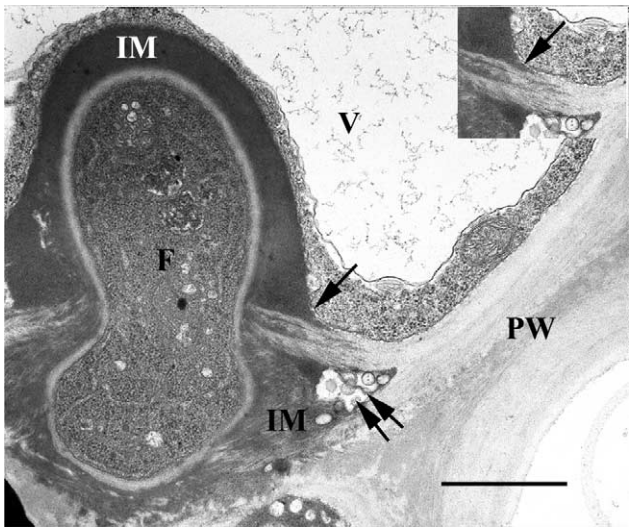

Fig. 2. Transmission electron micrograph of a compatible interactions between *U. hordei* and barley, 6 dpi. Fungal mycelium grew into the bundle sheath cells showing a hypha within a parenchyma cell. Note the thick interfacial matrix, which had infiltrated into the intercellular space. The plant plasma membrane was continuous (single arrow). Electron-transparent vesicles could be seen in the intercellular space (double arrows). Scale bar = 1 μM. Abbreviations as in Fig. 1.

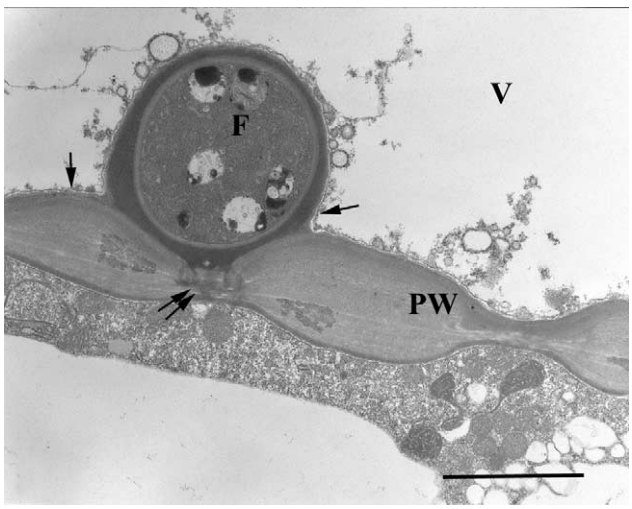

Fig. 3. Transmission electron micrograph of a compatible interactions between *U. hordei* and barley, 6 dpi. Fungal fragment in a plant bundle sheath cell bordering a developing vessel cell. Note the electron-dense substance of the interfacial matrix infiltrating the plant cell wall (double arrows). The plant plasma membrane was continuous (single arrow). Scale bar = 2·5 μM. Abbreviations as in Fig. 1.

Plant mitochondria, nuclei, endoplasmic reticula and Golgi bodies were found to be closely associated with and aggregated near hyphae (Figs. 9 and 10). Interestingly, at 12 dpi, tubule-like structures, varying in length and orientation, seemed to have developed in the outer region of the interfacial matrix (Figs. 11 and 12).

3.2. Incompatible interaction between barley and U. hordei; localized HR

The sequence of events visible during the incompatible interaction brought about by the combination of the fungal avirulence gene, *V1*, and the *Ruh1* resistance gene in barley cultivar 'Hannchen', was dramatically different. A very

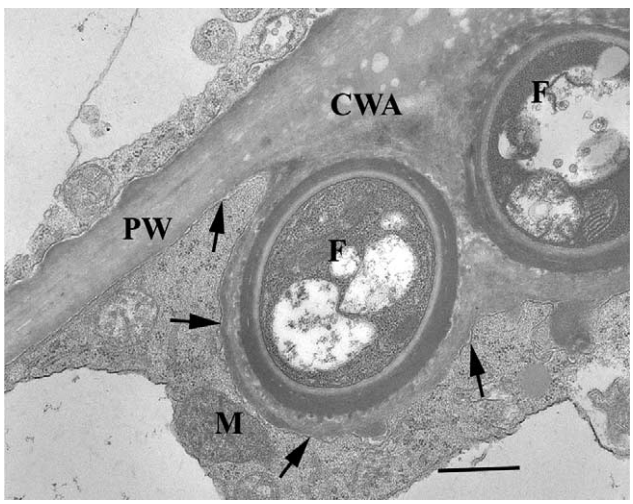

Fig. 4. Transmission electron micrograph of a compatible interactions between *U. hordei* and barley, 12 dpi. Fungal hyphae encased by the host cell wall apposition. Plant plasma membrane was continuous (arrows). Scale bar = 1 μM. Abbreviations as in Fig. 1.

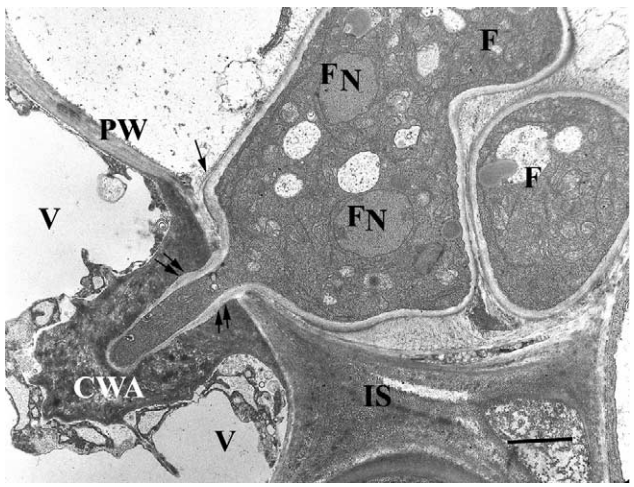

Fig. 5. Transmission electron micrograph of a compatible interactions between *U. hordei* and barley, 12 dpi. Hypha extending from one cell to another. This dikaryotic hypha did not have a discernable interfacial matrix (arrows) and was surrounded by a thick cell wall apposition (CWA), which apparently developed as a deposit on the inner surface of the plant cell wall. Scale bar = 2 μM. Abbreviations as in Fig. 1.

localized, cellular HR seemed to be elicited at very early time points during fungal invasion caused by this gene-for-gene combination. However, no macroscopic symptoms or necrosis can be observed. Mating on the shoot surface and direct penetration did not appear to be affected (data not shown). At 2 dpi, the infective mycelium induced from beneath the appressorium-like structure, penetrated into the epidermal cells (Fig. 13) but did not appear as healthy as that in compatible cells. For example, they seemed affected by early wall depositions and constrictions (Figs. 13–15, compare Figs. 1–6). The electron-opaque interfacial matrix was present around the penetrated hyphae (Figs. 13 and 14). As early as 2 dpi, thick cell wall appositions were deposited outside of the electron-opaque interfacial matrix encasing

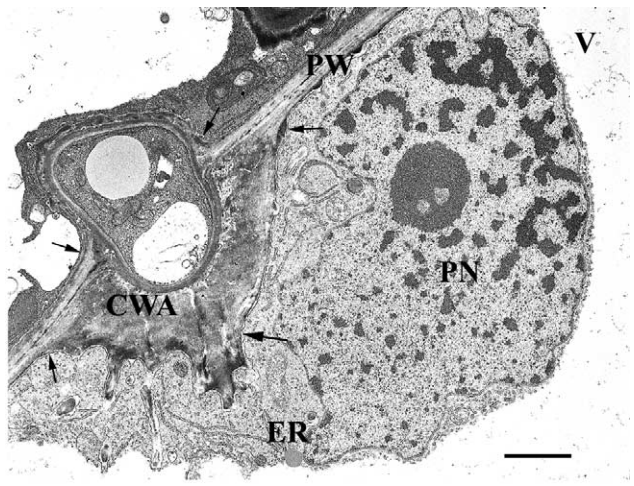

Fig. 6. Transmission electron micrograph of a compatible interactions between *U. hordei* and barley, 12 dpi. Thick cell wall appositions covered the fungal hypha. The plant cell wall was breached but the plasma membrane was continuous and convoluted (arrows). Scale bar = 2 μM. Abbreviations as in Fig. 1.

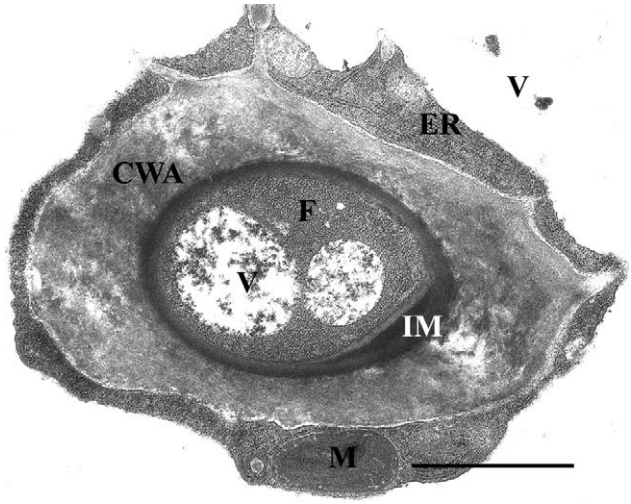

Fig. 7. Transmission electron micrograph of a compatible interactions between *U. hordei* and barley, 12 dpi. Higher magnification detailing the structure of the thick layer of cell wall apposition encasing the hypha in the plant cytoplasm. Note the electron-opaque interfacial matrix (IM). Scale bar = 2 μM. Abbreviations as in Fig. 1.

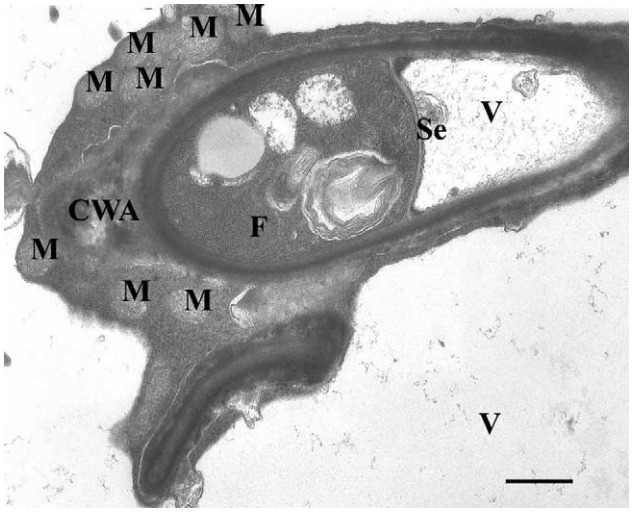

Fig. 9. Transmission electron micrograph of a compatible interactions between *U. hordei* and barley, 12 dpi. Multiple plant mitochondria (M) aggregated around the intracellular hypha, which was encased by cell wall apposition (CWA). A septum (Se) dividing the mycelium was visible. Scale bar = 1 μM. Abbreviations as in Fig. 1.

the penetrated hyphae (Figs. 14 and 15). Numerous amorphous vesicles were present in the region between interfacial matrix and cell wall apposition (Fig. 14). The cell wall apposition was seen in the neighboring epidermal cells, although no mycelium was found in these cells (Fig. 15). Many invaded epidermal cells, if not all, appeared disorganized with disintegrated cytoplasm showing numerous abnormal mitochondria, Golgi bodies, endoplasmic reticula and nuclei (Figs. 14 and 16). Numerous small, amorphous and electron-transparent structures were also observed in vacuoles of such epidermal cells. Dissolution of the plant cell wall was displayed at the penetration point (Figs. 14, 16 and 17). In a few cases, the growth of penetrating hyphae seemed arrested in the epidermal cell, blocking further extension to other plant cells (data not shown). Large amounts of electron-dense osmiophyllic material distinct from the interfacial matrix and possibly of plant origin were apparent in penetrated epidermal cells (Fig. 16). This material harbored electron-transparent amorphous vesicles and often these affected cells appeared necrotic (Fig. 16). Another substance, more fibrous in nature, possibly debris from the plant cell walls, which were separated by the growth of invaded fungus, was often found (Fig. 17). In addition, cell wall apposition was often found deposited on the cell wall of adjacent mesophyll cells (Fig. 17). However, in comparison to the material laid down

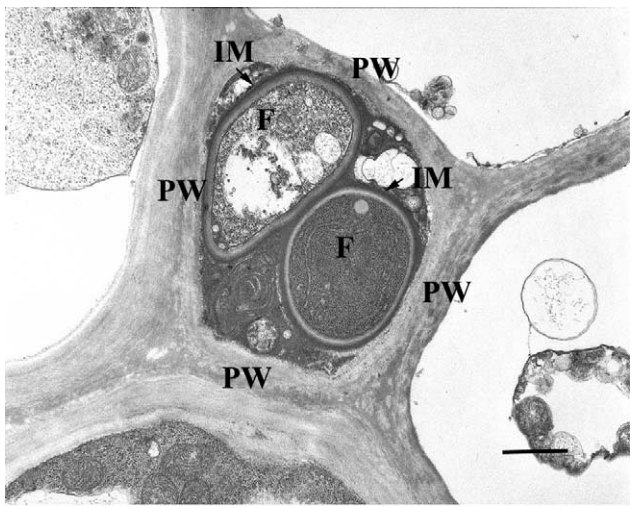

Fig. 8. Transmission electron micrograph of a compatible interactions between *U. hordei* and barley, 12 dpi. Two hyphae in the intercellular space, each surrounded by interfacial matrix. An electron-dense substance was filling the intercellular space. Scale bar = 1 μM. Abbreviations as in Fig. 1.

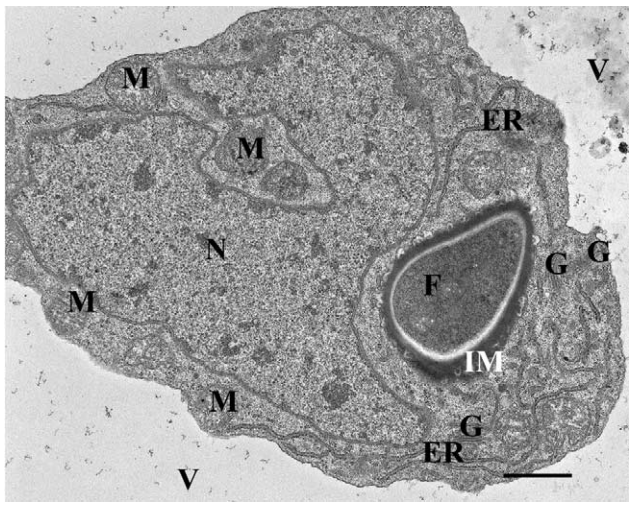

Fig. 10. Transmission electron micrograph of a compatible interactions between *U. hordei* and barley, 12 dpi. Hyphae that extended in host cells were closely associated with the plant cell nucleus (PN), endoplasmic reticula (ER) and Golgi bodies (G). Scale bar = 1 μM. Abbreviations as in Fig. 1.

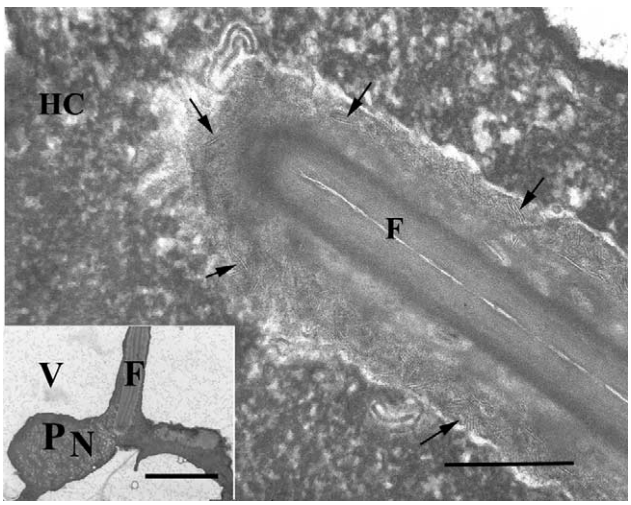

Fig. 11. Transmission electron micrograph of a compatible interactions between *U. hordei* and barley, 12 dpi. Inset: a longitudinal section of a hypha in plant cytoplasm. Note the close proximity of the plant cell nucleus (PN). Scale bar = 5 μM. Main frame: numerous tubule-like structures were present in the interfacial matrix between plant cytoplasm and hypha (arrows). These tubule-like structures were orientated in all directions. Scale bar = 0·5 μM. Abbreviations as in Fig. 1.

during compatible interactions, the cell wall appositions invoked by this resistance reaction appeared thicker and of a more granular nature (compare Figs. 4 and 7).

At 6 dpi, both inter- and intracellular hyphae were present in mesophyll cells (Figs. 18–20). A thick layer of granular-appearing cell wall apposition was found surrounding the hyphae in mesophyll cells (Figs. 20 and 21). Tubule-like structures frequently appeared in the region outside the interfacial matrix, along the invading hyphae (Fig. 18, inset). Intercellular hyphae were surrounded by an electron-dense matrix containing electron-transparent vesicles (Fig. 19). Cell wall appositions appeared to be closely

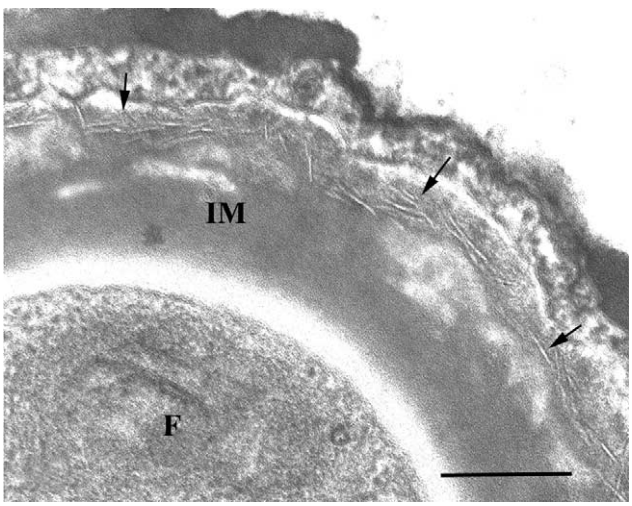

Fig. 12. Transmission electron micrograph of a compatible interactions between *U. hordei* and barley, 12 dpi. High magnification of a transverse section through a hypha in a plant cell. Tubule-like structures (arrows) are clearly visible localized mainly in the outer region of the interfacial matrix. Scale bar = 0·5 μM. Abbreviations as in Fig. 1.

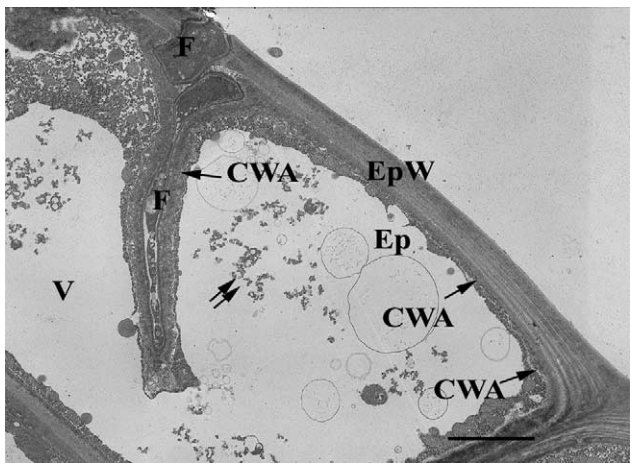

Fig. 13. Transmission electron micrograph of an incompatible interactions between *U. hordei* and barley, 2 dpi. An infection hypha penetrated into a plant epidermal cell. The penetration hypha did not appear as healthy in comparison to those seen in compatible interactions. Scattered amorphous material was visible in the vacuole of the epidermal cell (double arrows). Cell wall apposition (CWA) surrounded all penetrating hyphae and extended to cover the whole inner surface of the epidermal cell. Scale bar = 5 μM. Abbreviations as in Fig. 1.

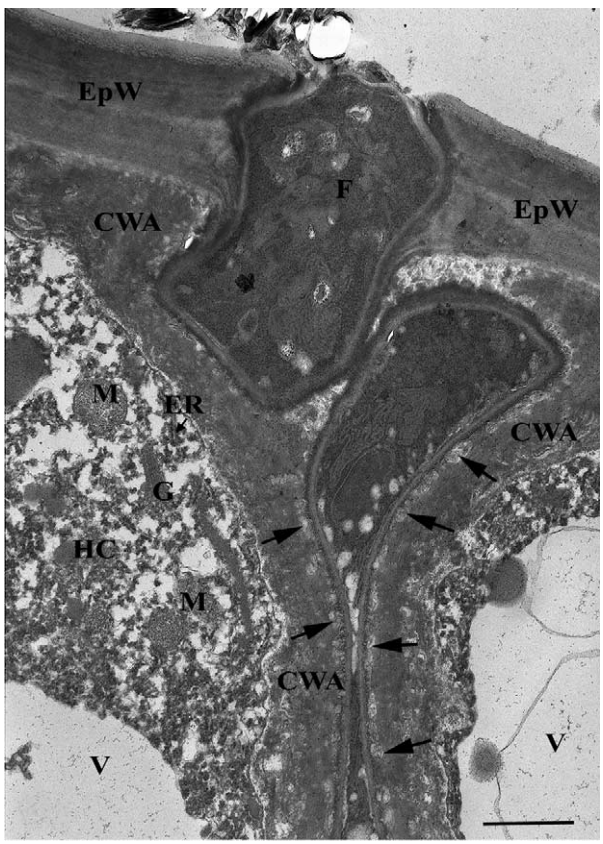

Fig. 14. Transmission electron micrograph of an incompatible interactions between *U. hordei* and barley, 2 dpi. Enlargement of Fig. 13. Numerous electron-transparent vesicles (arrows) could be seen in between the interfacial matrix and cell wall apposition. Plant mitochondria, endoplasmic reticula, Golgi bodies and cytoplasm were disintegrated. Note host cell organelles in close proximity to the hypha, and granular-appearing host cytoplasm. Scale bar = 1 μM. Abbreviations as in Fig. 1.

associated with vesicles, mitochondria and ER in the invaded plant cytoplasm (Figs. 20–22). Plant plasma membranes of necrotic cells became dislocated from the plant cell wall exhibiting much disruption (Fig. 20). Corresponding hyphae appeared necrotic and degraded (Figs. 21–23). Disrupted plant cells exhibited disintegrated nuclei and vesicles in the degrading cytoplasm (Figs. 21 and 22). Moreover, the texture of cell wall appositions in necrotic plant cells appeared different from that in compatible interactions (Figs. 21 and 23). In some cases, a layer containing a dense fibrous substance appeared around the degrading hyphae in necrotic cells (Fig. 23).

4. Discussion

Here we provide a detailed, ultrastructure comparative analysis of cell morphologies during early steps of the infection process in a compatible and an incompatible interaction. The latter is most likely the result of the effects of an epistatic fungal avirulence gene (product), which is recognized by its cognate plant host resistance gene (product). Traditional disease severity ratings consider a reaction between a *U. hordei* race and a barley cultivar in which 0–5% of the plants show disease symptoms (smutted spikes), 'resistant'. When 5–35% of the plants become infected, the reaction is called 'intermediate', and levels greater than 36% are rated as 'fully susceptible' [35]. In this rating, the first category represents 'field resistance' which is not appropriate for geneticists studying gene-for-gene interactions. In our study, the *U. hordei* isolate carrying the avirulence gene *V1* has never produced teliospores on cultivar 'Hannchen' and the incompatibility has been shown to result from the epistatic interaction of dominant avirulence and resistance genes ([8,30,31,37]; Bakkeren, unpublished). The strains used for the compatible and incompatible inoculum, although not isogenic, share an extensive genetic background having been crossed at least four times. Because selection of progeny was based on the presence of avirulence gene *V1*, the events we observe in the incompatible interaction can most likely be attributed to the effects of this gene.

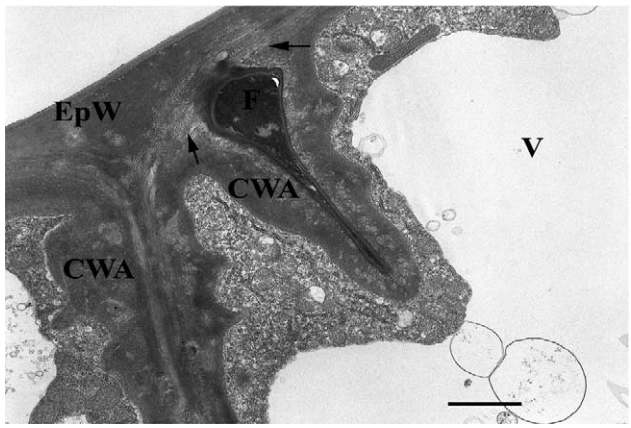

Fig. 15. Transmission electron micrograph of an incompatible interactions between *U. hordei* and barley, 2 dpi. There was deposition in the epidermal cell adjacent to the apposition in the invaded cell, although no hypha was observed in that cell. Note the electron-transparent vesicles around the infection hypha in the invaded cell (arrows). Scale bar = 4 μM. Abbreviations as in Fig. 1.

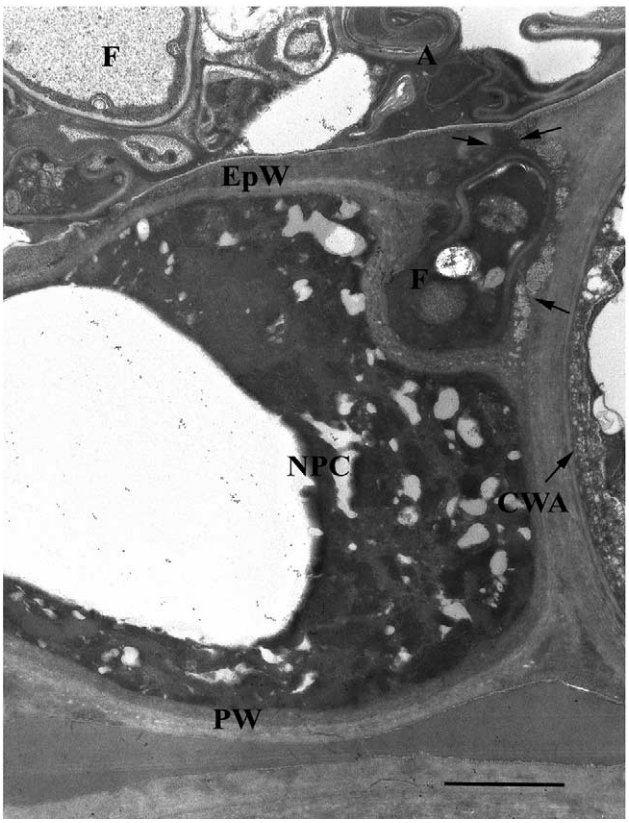

Fig. 16. Transmission electron micrograph of an incompatible interactions between *U. hordei* and barley, 2 dpi. An osmiophillic and electron-opaque substance filled most of the invaded epidermal cell, presumably indicating epidermal cell necrosis. Cell wall apposition occurred in neighboring epidermal cells (arrow). Scale bar = 2 μM. Abbreviations as in Fig. 1.

The pathogenic dikaryon penetrated the coleoptile of the germinating barley seedling directly regardless of whether the host was resistant or susceptible. Presumably the avirulence gene *V1* product is not yet recognized by host cell components at this stage. As soon as epidermal cells were invaded, an interfacial matrix of electron-opaque material was laid down between the invading fungal hyphal wall and the invaginated plasma membrane of the plant cell and this process occurred in both compatible and incompatible interactions. It appeared that this matrix thickened during later stages of fungal development. Such a matrix was also reported for other Ustilaginales [5,6,25,28,32,33]. The biological significance, biochemical make-up and origin of this matrix could not be determined in our studies.

A striking feature of the host reaction to an incompatible *U. hordei* infection was the formation of cell wall

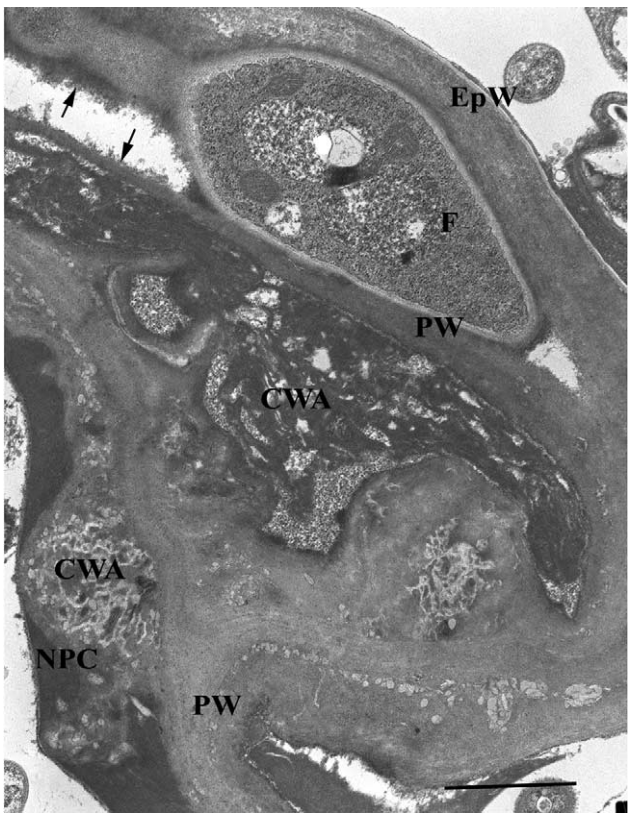

Fig. 17. Transmission electron micrograph of an incompatible interactions between *U. hordei* and barley, 2 dpi. Fibrous material (arrows), possibly the residues from the plant cell wall, existed close to the hypha within a plant cell. Cell wall apposition (CWA) was deposited in a presumed corner of a collapsed plant cell and in the inner surface of adjacent cell, and had a granular appearance. Scale bar = 2 μM. Abbreviations as in Fig. 1.

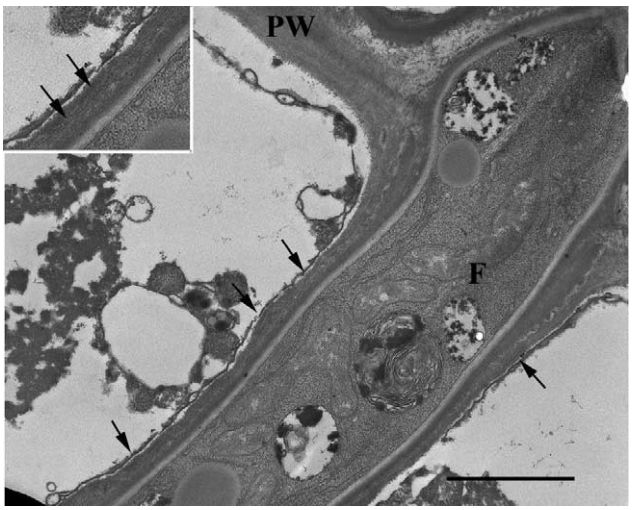

Fig. 18. Transmission electron micrograph of an incompatible interactions between *U. hordei* and barley, 6 dpi. Fungal hypha (F) extending from one cell to another. Tubule-like structures were present along the fungal hypha between the interfacial matrix and plant cell plasma membrane; see arrows in inset at higher magnification. Note the plant cell plasma membrane separated from the cell wall (arrows) and numerous electron-dense spherical structures present in the plant vacuole. Scale bar = 2 μM. Abbreviations as in Fig. 1.

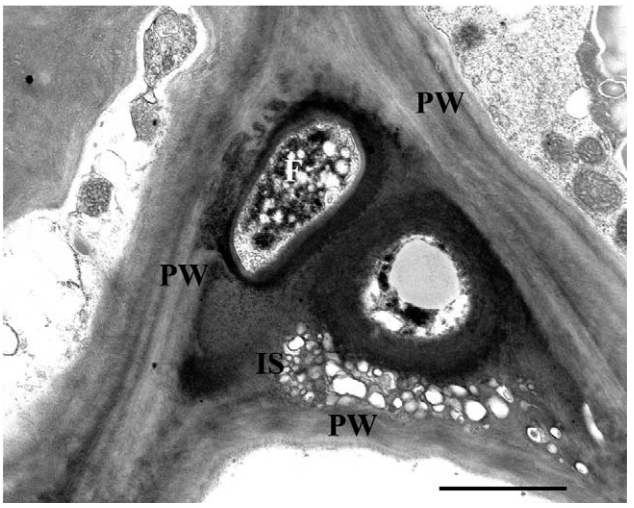

Fig. 19. Transmission electron micrograph of an incompatible interactions between *U. hordei* and barley, 6 dpi. Highly disorganized and necrotic intercellular hyphae (F) were encased in osmiophillic material. Scale bar = 2 μM. Abbreviations as in Fig. 1.

appositions at sites of fungal penetration and/or adjacent cell walls, as early as 2 days after inoculation. This suggests that actual contact between fungal and plant cells (that is, after epidermal penetration) is needed for the resistance reaction to be initiated. It is as yet unknown whether the fungal avirulence gene product is excreted or wall bound and how this factor is perceived by the host cell (with the aid of the cognate *Ruh1* resistance gene). These cell wall appositions are usually large, numerous, associated with degrading fungal mycelia, and may create a mechanical barrier preventing the fungus from further ingression in the inner tissues. In compatible interactions, cell wall appositions are also observed but only at later stages of development and

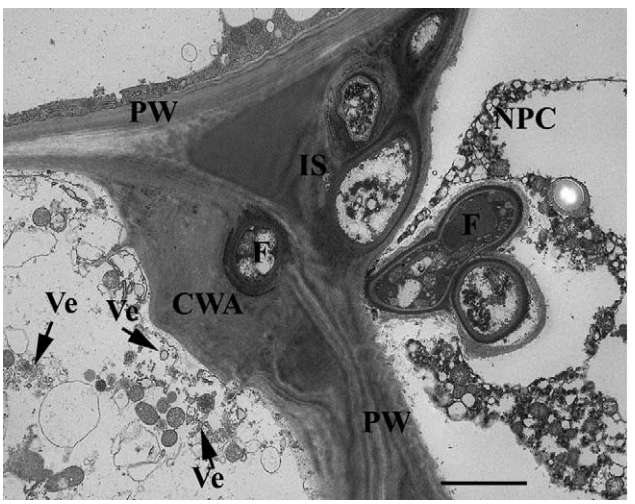

Fig. 20. Transmission electron micrograph of an incompatible interactions between *U. hordei* and barley, 12 dpi. Cell wall apposition appeared to be associated with numerous vesicles (Ve). Note the necrotic and partially plasmolyzed right-hand cell (NPC). Scale bar = 5 μM. Abbreviations as in Fig. 1.

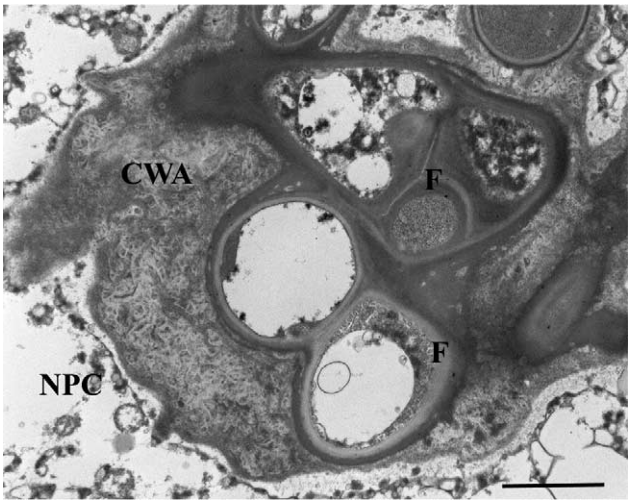

Fig. 21. Transmission electron micrograph of an incompatible interactions between *U. hordei* and barley, 12 dpi. Necrotic hyphae (F) encased by cell wall apposition in an apparent necrotic cell. Structures of granular appearance could be seen in the cell wall apposition. Scale bar = 2 μM. Abbreviations as in Fig. 1.

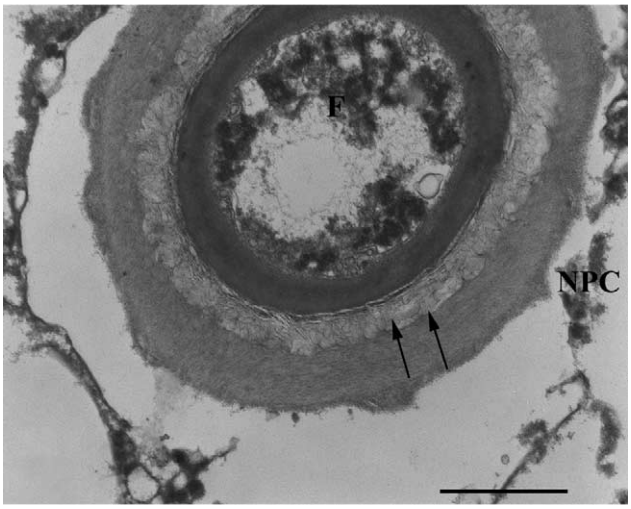

Fig. 23. Transmission electron micrograph of an incompatible interactions between *U. hordei* and barley, 12 dpi. An apparent necrotic hypha in a necrotic plant cell. Dense tubule-like structures (arrows) were present between the interfacial matrix and presumably the cell wall apposition. Scale bar = 1 μM. Abbreviations as in Fig. 1.

form on the inner surface of the host cell wall opposite to the point of hyphal penetration as seen for other cereal smuts [25]. Continued deposition of wall material around the invading hyphae resulted in a cell wall apposition very similar to the type II collar in rust fungi [24]. In addition to a difference in time of appearance, our study showed that the apposition texture differed between compatible and incompatible interactions. A more granular-appearing substance could be seen in incompatible cell wall appositions, however, no direct evidence that this prevented penetration was observed. The biochemical composition of these cell wall appositions could not be determined using conventional electron microscopy. Chatterjee [7] reported that microchemical testing revealed cellulose in the 'sheath-like structures' which could not be induced by mechanical wounding. Kiesling [19] reported a difference in chemical staining of this 'sheath' between compatible and incompatible interactions (thionin or Lauth's violet in Conant stain) leading him to postulate a 'chemical' resistance response. Recently developed immunoelectron microscopy and molecular localization techniques may be useful in elucidating its components and possible function.

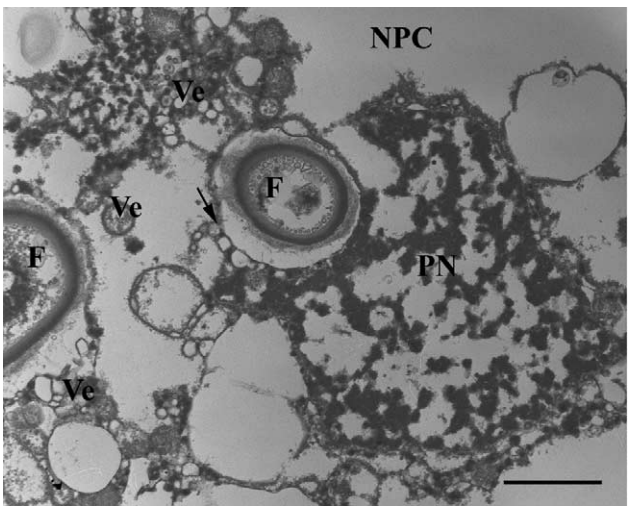

Fig. 22. Transmission electron micrograph of an incompatible interactions between *U. hordei* and barley, 12 dpi. Disorganized fungal hyphae (F) in a necrotic plant cell. The plant nucleus and cytoplasm both were highly disorganized. Scale bar = 2 μM. Abbreviations as in Fig. 1.

Cell wall apposition (containing β-1,3-glucanases) was also found lining necrotic host cells that had been invaded by an early haustorium of an incompatible race of the wheat leaf rust fungus, *Puccinia triticina* [16]. Also in this interaction, direct cell-to-cell contact was necessary to trigger this response, because events during infection through stomata and occupation of the substomatal cavity were indistinguishable between compatible and incompatible combinations. However, fungal cells were not enveloped in an interfacial matrix nor did they become encased [16,29]. There was also no encasement of powdery mildew (*Blumeria graminis* f. sp *hordei*) hyphae entering incompatible barley leaf cells, although papillae were formed on the inner cell wall around sites of direct penetration [2,20]. Papillae were formed in both compatible and incompatible interactions but were larger in the latter case. It is unknown whether these papillae relate to the wall apposition we described e.g. in terms of composition. In another cereal pathosystem, the direct penetration via appressoria of sorghum cells by incompatible *Colletotrichum sublineolum*, led also to large papillae at the penetration sites [41]. However, in this case infection vesicles became encased in a highly electron-opaque material leading to their death.

Tubule-like structures were found in the region between the interfacial matrix and the layer of cell wall apposition in both compatible and incompatible *U. hordei*/barley interactions. However, these tubules seemed to be denser and appeared earlier in the latter interaction. This ultrastructural phenomenon has never been reported in other Ustilaginales before. Its origin and biological significance are unknown.

The HR of a resistant host to pathogen infection is characterized by disorganization and rapid death (necrosis) of cells at the infection site. This reaction is correlated with an orchestrated series of events called programmed cell death, and is caused by the activation of an integral but specific genetic complement of genes. It is a typical feature of many pathosystems displaying race/cultivar-specific resistance (for example see [13,18,22]). Depending on the pathosystem, necrotic lesions resulting from a HR at sites of infection may contain from one to many brown, dead cells, but are often clearly visible. We observed only very localized necrosis (up to 2–3 cells) after 2 days after inoculation in the incompatible interaction, when penetrating hyphae made contact with the cytoplasm of epidermal cells. This necrosis displayed typical features of a HR/hypersensitive cell death. A molecular analysis of genes and factors typically involved in a HR will be needed to support our findings. The Gramineae-infecting pathogens mentioned before, *Puccinia triticina*, *Blumeria graminis* f. sp *hordei* and *Colletotrichum sublineolum*, caused a necrotic reaction in incompatible host cells immediately upon penetration. Cell death was limited to the invaded cell, although in sorghum neighboring cells were seen to accumulate pigmented vesicles. The timing of these events within 48 h in all these pathosystems was roughly similar to the one we described for the incompatible *U. hordei*/barley interaction.

Resistance can be expressed as an early, total obstruction of pathogen ingress beyond the first or second cell in highly resistant cultivars. This seems to be the case in our system presumably triggered by the presence of the avirulence gene, *V1*. It seems that in genuine gene-for-gene interactions in which single dominant genes dictate a fully incompatible *U. hordei*/barley interaction, that is, when cultivars never produce smutted spikes under different environmental conditions, resistance involves a rapid encasement of invading hyphae and induction of local necrosis of only invaded cells and their immediate neighbors. This had been reported previously in general terms using light microscopic analysis in the case of infection with *U. hordei*, race 6 (not harboring *V1*) on cultivars 'Pannier' and 'Jet' [7,19]. During the majority of interactions, an intermediate resistance response is obtained during which variable percentages of smutted plants will be seen depending on environmental conditions. In this case, resistance often seems to be inherited in a polygenic fashion resulting in the containment of some invading mycelium in the first invaded cells of the epidermis. Further advance in the seedling seems to be checked by a restriction of the size and mass of hyphae leading to mycelial death without a visible cytoplasmic reaction of host cells, although this has not been verified on an ultrastructural level. Kiesling [19] and Chatterjee [7] reported that, in addition, when other seedlings were sectioned during these combinations, hyphae could be seen growing as in susceptible interactions. Conceivably, this could lead to the occasional 'escape' and low percentages of smutted plants. Curiously, they reported that, even in susceptible varieties, coleoptilar cells were found collapsed in areas of heavy inoculum. Necrosis of plant cells during compatible *U. hordei*–barley interactions was never observed in our system. Fungal mycelium can be detected either microscopically or by PCR in most if not all inoculated cultivars independent of their disease rating although not in all tissues or developmental stages of the host [11,12,42]. It would be very informative to compare the timing, localization and kind of host cellular resistance response on an ultrastructural level triggered by different gene-for-gene combinations.

The HR has been proposed to play an important role in resistance in that host cell death is thought to deprive the pathogen of nutrients, resulting in pathogen containment. In addition, HR-affected cells might also send out signals to sensitize nearby cells and heighten resistance systemically in the whole plant [13,29]. Our study indicates that there is a strong correlation between resistance and host cell death. However, it was not shown that in the incompatible interaction the necrotic host cell reactions alone could halt the growth of hyphae into adjacent cells. Indeed, as mentioned before, intermediate resistance in the *U. hordei*/barley pathosystem was achieved by restricting the growth of hyphae without an obvious visible host cytoplasmic reaction. In many host-pathogen systems investigators have yet to correlate conclusively host cell necrosis with fungal resistance and hyphal death [22]. It would be interesting to compare these reactions, the time of appearance and structure of cell wall appositions, potential disorganization of fungal and host cytoplasm, and the formation of tubule-like structures, in interactions resulting from invading hyphae of 'inappropriate' smut fungi, such as *U. kolleri* (which is normally pathogenic on *Avenae* species). This would shed light on whether some of these reactions are solely triggered by avirulence gene products or whether they can represent a more general non-host resistance reaction [14]. However, it is conceivable that smut species closely related to *U. hordei* (in the small grain-infecting group) harbor species-specific avirulence genes that could trigger similar responses.

In summary, the resistance of barley cultivars harboring the resistance gene *Ruh1*, to *U. hordei* carrying the cognate avirulence gene *V1*, is characterized by the induction of structural barriers such as the formation of host cell wall appositions, by the encasement and necrosis of hyphae, and by the disintegration of invaded host cells and possibly their immediate neighbors as soon as the first epidermal cell has

been invaded. This gene-for-gene resistance is therefore associated with a rapid, active and very localized hypersensitive host cell death (HR), which limits the rate and extent of fungal colonization in the host tissues. It is unclear whether this HR alone is preventing stele colonization. We are currently unraveling the molecular basis triggering this chain of events and are analyzing other *Avr*/*R* gene-for-gene combinations at the ultrastructural level.

Acknowledgements

We gratefully appreciate the technical assistance by Michael Weis and thank Drs H. Sanfaçon and K. Snetselaar for valuable comments on the manuscript.

References

[1] Abdennadher M, Mills D. Telomere-associated RFLPs and electrophoretic karyotyping reveal lineage relationships among race-specific strains of *Ustilago hordei*. Current Genetics 2000;38:141–7.
[2] Aist JR, Bushnell WR. Invasion of plants by powdery mildew fungi, and cellular mechanisms of resistance. In: Cole GT, Hoch HC, editors. The Fungal Spore and Disease Initiation in Plants and Animals. New York: Plenum; 1991. p. 321–45.
[3] Anderson CM, Willits DA, Kosted PJ, Ford EJ, Martinez-Espinoza AD, Sherwood JE. Molecular analysis of the pheromone and pheromone receptor genes of *Ustilago hordei*. Gene 1999;240: 89–97.
[4] Bakkeren G, Kronstad JW. Linkage of mating-type loci distinguishes bipolar from tetrapolar mating in basidiomycetous smut fungi. Proceedings of the National Academy of Sciences, USA 1994;91: 7085–9.
[5] Bauer R, Mendgen K, Oberwinkeler F. Cellular interaction of the smut fungus *Ustacystis waldsteiniae*. Canadian Journal of Botany 1995;73:867–83.
[6] Bauer R, Oberwinkler F, Vanky K. Ultrastructural markers and systematics in smut fungi and allied taxa. Canadian Journal of Botany 1997;75:1273–314.
[7] Chatterjee P. 1956. Nature of resistance to penetration and infection of *Ustilago hordei* (Pers.) Lagerh. In seedlings of four hull-less spring barley varieties. PhD Thesis, Michigan State University, East Lansing, M
[8] Ebba T, Person C. Genetic control of virulence in *Ustilago hordei*. IV. Duplicate genes for virulence and genetic and environmental modification of a gene-for-gene relationship. Canadian Journal of Genetics and Cytology 1975;17:631–6.
[9] Fisher GW, Holton CS. Biology and control of the smut fungi. New York: Ronald Press; 1957. p. 622.
[10] Fullerton RA. An electron microscopic study of intracellular hyphae of some smut fungi. Australian Journal of Botany 1970;18:285–92.
[11] Groth JV, Person CO. Smutting patterns in barley and some plant growth effects caused by *Ustilago hordei*. Phytopathology 1978;68: 477–83.
[12] Groth JV, Person CO, Ebba T. The measurement of disease severity in cereal smut. In: Muhammed AR, Aksel R, von Borstel RC, editors. Genetic Diversity in Plant. New York: Plenum Press; 1977. p. 193–204.
[13] Heath MC. Hypersensitive response-related death. Plant Molecular Biology 2000;44:321–34.
[14] Heath MC. Cellular interactions between biotrophic fungal pathogens and host or nonhost plants. Canadian Journal of Plant Pathology 2002; 24:259–64.
[15] Hu GG, Rijkenberg FHJ. Ultrastructural studies of the intercellular hypha and haustorium of *Puccinia recondita* f.sp. *tritici*. Journal of Phytopathology 1998;146:39–50.
[16] Hu GG, Rijkenberg FHJ. Subcellular localization of β-1,3-glucanase in *Puccinia recondita* f.sp. *tritici*-infected wheat leaves. Planta 1998; 204:324–34.
[17] Hu GG, Linning R, Bakkeren G. Sporidial mating and infection process of the smut fungus, *Ustilago hordei*, in susceptible barley. Canadian Journal of Botany 2002;80:1103–14.
[18] Huang C, Groot T, Meijer-Dekens F, Niks RE, Lindhout P. The resistance to powdery mildew (*Oidium lycopersicum*) in *Lycopersicon* species is mainly associated with hypersensitive response. European Journal of Plant Pathology 1998;104:399–407.
[19] Kiesling R.L. 1952. Histological studies on covered smut of barley. PhD Thesis, University of Wisconsin, Madison, Wisconsin
[20] Kita N, Toyoda H, Shishiyama J. Chronological analysis of cytological responses in powdery-mildewed barley leaves. Canadian Journal of Botany 1981;59:1761–8.
[21] Kozar F. The pathway of infection of *Ustilago hordei*. Canadian Journal of Genetics and Cytology 1969;11:977–86.
[22] Lam E, Kato N, Lawton M. Programmed cell death, mitochondria and the plant hypersensitive response. Nature 2001;411:848–53.
[23] Lee N, Bakkeren G, Wong K, Sherwood JE, Kronstad JW. The mating type and pathogenicity locus of the fungus *Ustilago hordei* spans a 500-kb region. Proceedings of the National Academy of Sciences, USA 1999;96:15026–31.
[24] Littlefield LJ, Heath MC. Ultrastructure of Rust Fungi. New York: Academic Press; 1979. p. 277.
[25] Luttrell ES. Relations of hyphae to host cells in smut galls caused by species of *Tilletia*, *Tolyposporium* and *Ustilago*. Canadian Journal of Botany 1987;65:2581–91.
[26] Martinez-Espinoza AD, Gerhardt SA, Sherwood JE. Morphological and mutational analysis of mating in *Ustilago hordei*. Experimental Mycology 1993;17:200–14.
[27] Mathre DE. Compendium of barley diseases. St. Paul, MN: American Phytopathological Society Press; 1997.
[28] Mims CW, Snetselaar KM, Richardson EA. Ultrastructure of the leaf stripe smut fungus *Ustilago striiformis*: host-pathogen relationship and teliospore development. International Journal of Plant Sciences 1992;153:289–300.
[29] Niks RE, Dekens RG. Prehaustorial and posthaustorial resistance to wheat leaf rust in diploid wheat seedlings. Phytopathology 1991;81: 847–51.
[30] Sidhu G, Person C. Genetic control of virulence in *Ustilago hordei*. II. Segregations for higher levels of virulence. Canadian Journal of Genetics and Cytology 1971;13:173–8.
[31] Sidhu G, Person C. Genetic control of virulence in *Ustilago hordei*. III. Identification of genes for host resistance and demonstration of gene-for-gene relations. Canadian Journal of Genetics and Cytology 1972;14:209–13.
[32] Snetselaar KM, Mims CW. Infection of maize stigmas by *Ustilago maydis*: Light and electron microscopy. Phytopathology 1993;83: 843–50.
[33] Snetselaar KM, Mims CW. Light and electron microscopy of *Ustilago maydis* hyphae in maize. Mycological Research 1994;98:347–55.
[34] Spurr AR. A low-viscosity epoxy resin embedding medium for electron microscopy. Journal of Ultrastructural Research 1969;26: 31–43.
[35] Tapke VF. Physiologic races of *Ustilago hordei*. Journal of Agricultural Research 1937;55:683–92.
[36] Tapke VF. New physiologic races of *Ustilago hordei*. Phytopathology 1945;35:970–6.
[37] Thomas PL. Interaction of virulence genes in *Ustilago hordei*. Canadian Journal of Genetics and Cytology 1976;18:141–9.

[38] Thomas PL, Kim WK, Howes NK. Independent inheritance of genes governing virulence and the production of a polypeptide in *Ustilago hordei*. Journal of Phytopathology 1987;120:69–74.
[39] Thomas PL. Genetics of small grain smuts. Annual Review of Phytopathology 1991;29:137–48.
[40] Thomas PL, Menzies JG. Cereal smuts in Manitoba and Saskatchewan 1989–95. Canadian Journal of Plant Pathology 1997;19:161–5.
[41] Wharton PS, Julian AM, O'Connell RJ. Ultrastructure of the infection of *Sorghum bicolor* by *Colletotrichum sublineolum*. Phytopathology 2001;91:149–58.
[42] Willits DA, Sherwood JE. Polymerase chain reaction detection of *Ustilago hordei* in leaves of susceptible and resistant barley varieties. Phytopathology 1999;89:212–7.